Time-frequency analysis of electroencephalogram series. III. Wavelet packets and information cost function

S. Blanco,[1,*] A. Figliola,[1,†] R. Quian Quiroga,[2,‡] O. A. Rosso,[1,§] and E. Serrano[3]
[1]*Facultad de Ciencias Exactas y Naturales, Instituto de Cálculo, Universidad de Buenos Aires, Pabellón II, Ciudad Universitaria, 1428 Buenos Aires, Argentina*
[2]*Institute of Physiology, Medical University Lübeck, Ratzeburger Alle 160, D-23538 Lübeck 1, Germany*
[3]*Departamento de Matemática, Facultad de Ciencias Exactas y Naturales, Universidad de Buenos Aires, Pabellón I, Ciudad Universitaria, 1428 Buenos Aires, Argentina*
(Received 10 June 1997; revised manuscript received 19 August 1997)

Signals obtained during tonic-clonic epileptic seizures are usually neglected for analysis by the physicians due to the presence of noise caused by muscle contractions. Although noise obscures completely the recording, some information about the underlying brain activity can be obtained with wavelet transform by filtering those frequencies associated with muscle activity. One great advantage of this method over traditional filtering is that the filtered frequencies do not modify the pattern of the remanent ones. An accurate analysis of the different seizure stages was achieved using the wavelet packet method, and through the information cost function the brain dynamical behavior can be accessed. [S1063-651X(97)09712-2]

PACS number(s): 87.90.+y, 02.70.Hm

I. INTRODUCTION

The electroencephalogram (EEG) can be raftly defined as the mean electrical activity of the brain in different sites of the head. EEG patterns are correlated with functions, dysfunctions, and diseases of the central nervous system based on an empirical basis. Then clinical interpretation of EEG records are achieved by associating pathology characteristics (clinical symptomatology) with the visual inspection and pattern recognition of the EEG. Although this traditional analysis is quite useful, the visual inspection of the EEG is subjective, and hardly allows any systematization [1–4]. In order to overcome this, quantitative EEG analysis introduces objective measures reflecting the characteristics of the brain activity as well as the associated dynamics. However, we must remark that these methods are not developed for replacing traditional EEG visual analysis, but rather they complement them as additional tools.

Quantitative EEG analysis as a field includes a wide variety of techniques. These are frequency decomposition (spectral analysis), topographic mapping, compressed spectral arrays, significance probability mapping, and other complex analytical techniques [1–4]. A new approach to the problem of the quantification of the EEG series was achieved with nonlinear dynamics [5–11].

EEG's are complex signals whose statistical properties depends on both space and time. Regarding temporal characteristics, EEG signals are chaotic [5–11] and highly nonstationary (nevertheless, they can be analytically subdivided into short representative epochs where stationarity hypothesis is accomplished [9–11]).

Recently, we introduced two different techniques that allowed an analysis of an EEG time series in the time-frequency domain. The first was based on the Gabor transform [10,12–14], and the second one on the wavelet transform [15]. In the present work we present two significant improvements to the time-frequency analysis of the EEG series using wavelet transform. The first improvement is the introduction of the wavelet packet analysis [16]. The second improvement is the introduction of the information cost function (ICF), defined in terms of the wavelet coefficients, and essentially representing a Shannon entropy function [17,18]. We would like to remark that the applicability of these methods are not restricted only to EEG recordings.

Until the introduction of long term monitoring, spontaneous seizure EEG's were obtained only in those lucky situations in which the patient had a seizure during the few minutes of the recording. Normally, interictal EEG's (EEG's without seizure activity) were analyzed looking for pathological characteristics such as spikes, paroxysms, low frequency activity, etc. During those interictal EEG's, seizures were activated with photoestimulation, hyperventilation, and other clinical methods. However, provoked seizures do not necessarily have the same behavior as spontaneous ones. In order to overcome this limitation, long term video-EEG monitoring systems were developed. With video-EEG, after days of recording, clinical and electroencephalographic information can be correlated for obtaining an accurate evaluation of the seizures. Seizure starting, duration, post-seizure recovering, classification of the seizure, and different stages are some of the characteristics usually analyzed. However, in the case of tonic clonic seizures, muscle activity provoked by violent movements completely obscures the EEG recordings, limiting the analysis only to the starting and the post-seizure stages. Visual inspection of the EEG, and traditional mathematical methods such as Fourier transform are no longer applicable in these cases, owing to the great amount of noise involved. In consequence, brain activity during this kind of

*Electronic address: blanco@ulises.ic.fcen.uba.ar
†Electronic address: figliola@ulises.ic.fcen.uba.ar
‡Electronic address: rodri@physio.mu-luebeck.de
§Electronic address: rosso@ulises.ic.fcen.uba.ar

seizure has been observed only in special cases, for example in patients treated with ''curare'' (a drug that inhibits muscle responses) [19], or by filtering the signal in the frequency range of the muscle activity with standard methods [20]. However, filtering has several disadvantages, because it is impossible to separate brain and muscle activity and, further, it is well known that filtering high frequencies also affects the morphology of the low ones.

The aims of this work are to study a tonic clonic seizure, avoiding noise related limitations, by using wavelet transform and derived magnitudes in order to help physicians to identify and characterize the dynamical stage of the seizure as a complement of the video-EEG. The paper is organized in the following way. In Sec. II the clinical data and the experimental setup are presented. In Sec. III the time-frequency method based on wavelet transform is reviewed. The wavelet packets, as well as the information cost function, are introduced. In Sec. IV the analysis of a scalp EEG time series corresponding to an epileptic seizure is performed. Finally, in Sec. V a summary is given.

II. EXPERIMENTAL SETUP AND CLINICAL DATA

A scalp EEG signal is a nonstationary time series that usually presents artifacts due to an electrooculogram, an electromyogram, an electrocardiogram (ECG), and others [1–4]. Artifacts make a mathematical analysis of scalp EEG signals difficult. Sometimes, artifacts are presented for a few seconds, and can be obviated because they obscure only a small portion of the total EEG. In other cases, almost the total signal appears noisy and obscured by them, and very little information about the underlying brain activity can be extracted. An example of this kind of scalp EEG signal is the one corresponding to a tonic-clonic seizure [3].

A tonic-clonic ''grand mal'' seizure normally lasts around 40–90 s, and is characterized by violent muscle contractions. Initial massive tonic spasms are supplanted some seconds later by a clonic phase, with violent flexor movements and characteristic rhythmic spasms that last until the ending of the seizure.

Samples of EEG time series corresponding to generalized tonic-clonic seizures of epileptic patients were analyzed. Scalp and sphenoidal electrodes were applied following the 10-20 international system [1,2]. Each signal was digitized at 409.6 Hz through a 12 bit analog to digital converter, and filtered with an antialiasing eight pole low-pass Bessel filter with a cutoff frequency of 50 Hz. Then signals were digitally filtered with a 1–50-Hz bandwidth Butterworth filter and stored, after decimation, at 102.4 Hz in a personal computer hard drive. Recordings were done under video control in order to have an accurate determination of the different stages of the seizure. Analysis of each event included 1 min of EEG preseizure activity, and 2 min of the seizure and post-seizure phases. The different stages of EEG signals were determined by the physician team.

As an example, in Fig. 1 we present a scalp EEG signal, corresponding to a tonic-clonic epileptic seizure recorded in a central right location ($C4$ channel). In this record, the seizure starts at second 10, with a ''discharge'' of high frequencies. The tonic phase starts around second 35 with increasing amplitudes of the EEG, and the clonic phase begins around second 50 when the spasms dominates the EEG. The seizure clearly ends at second 85.

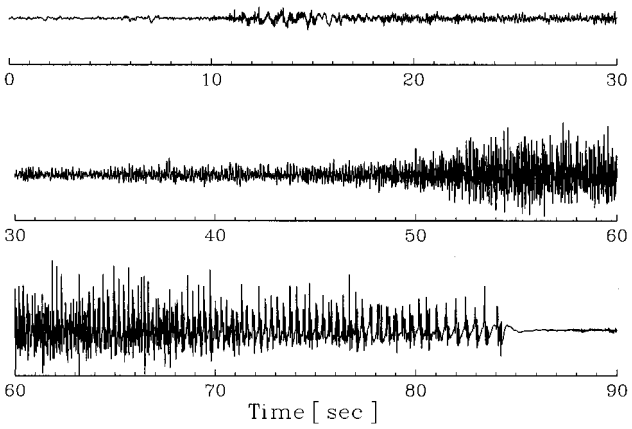

FIG. 1. Scalp EEG signal. Seizure starts at second 10, tonic phase at second 35, clonic phase at second 50. The seizure ends at second 85.

III. TIME-FREQUENCY ANALYSIS

A. Wavelet transform

Wavelet analysis gives us a powerful tool to confront very diverse problems in applied sciences or pure mathematics [21–27]. The wavelet is a smooth and quickly vanishing oscillating function with good localization both in frequency and time. It can be interpreted as single signals, or atoms, of short times with oscillating structures.

A wavelet family $\psi_{a,b}$ is the set of elemental functions generated by dilations and translations of a unique admissible mother wavelet $\psi(t)$,

$$\psi_{a,b}(t)=|a|^{-1/2}\psi\left(\frac{t-b}{a}\right), \tag{1}$$

where $a,b\in\mathbb{R},a\neq 0$ are the scale and translation parameters respectively, and t is the time. As a increases, the wavelet became more narrow. Thus we have a unique analystic pattern and its replicas at different scales and with variable localization in time.

Given a finite energy signal $S(t)$, the different correlations $\langle S,\psi_{a,b}\rangle$ indicate how precisely the wavelet function locally fits the signal at every scale a. This correlation operation defines the transformation that synthesizes the numerical information obtained in this way. From a different viewpoint, the wavelets of a family play the roles of elemental functions, representing the functions as a superpositions of wavelets correlated with the function for different scales (different a's). This makes it possible to organize the information in some particular structure to distinguish, for example, trends, or the shape associated with long scales of the local details from corresponding short scales.

The continuous wavelet transform of a signal $S(t)\in L^2(\mathbb{R})$ is defined as the correlation between the function $S(t)$ with the family wavelet $\psi_{a,b}$ for each a [23],

$$(W_\psi S)(a,\ b)=|a|^{-1/2}\int_{-\infty}^{\infty}S(t)\psi^*\left(\frac{t-b}{a}\right)dt=\langle S,\psi_{a,b}\rangle; \tag{2}$$

the asterisk denotes complex conjugation.

For special selections of the function, ψ and a discrete net of parameters $a_j=2^{-j}$ and $b_{j,k}=2^{-j}k$, with $j,k\in\mathbb{Z}$ and the scale 2^{-j}, give us the shift parameter. The subfamily

$$\psi_{j,k}(t)=2^{j/2}\psi(2^j t-k) \quad j,k\in\mathbb{Z}, \tag{3}$$

constitutes an orthonormal basis of the Hilbert space $L^2(\mathbb{R})$ [21,22]. In this way, we can obtain discrete transformations, and it is possible to expand the signal in a series of wavelets. Then we can join the advantages of the wavelet transform with the atomic decomposition of $S(t)$.

The discrete wavelet transform associated with ψ is simply seen as a restriction of the continuous wavelet transform at the parameter set $\{a_j,b_{j,k}\}$. In this case, as it is well known, the information given by the discrete wavelet transform can be organized according a hierarchical scheme of nested subspaces called the multiresolution analysis in $L^2(\mathbb{R})$ [21–24].

In the present analysis we used a multiresolution scheme based on cubic orthogonal spline functions as the mother wavelet, with a discretized version of the integral wavelet transform given by Eq. (2) [25]. We selected this wavelet due to the fact that it forms a base in $L^2(\mathbb{R})$ with a very convenient characteristic of symmetry and simplicity. Moreover, the smoothness of its derivatives are very suitable for representing natural phenomena.

In the following we will assume that the EEG signal is given by sampled values $\{s_0(n)\}$, $n=1,\ldots,M$, which correspond to a uniform time grid with sampling time Δt. Without loss of generality, we can suppose that the sampling rate is $\Delta t=1$. We define the representation of the signal by interpolating the sampled data in the form

$$S(t)=\sum_k s_0(k)\phi(t-k), \tag{4}$$

where $\phi(t)$ is the cubic cardinal spline, verifying $\phi(n)=\delta_{n0}$ [22].

For any resolution level $N<0$, we can write the decomposition of the signal as

$$S(t)=\sum_k s_N(k)\phi(2^N t-k)+\sum_{j=-N}^{-1}\sum_k C_j(k)\psi_{j,k}(t), \tag{5}$$

where $C_j(k)$ are the wavelet coefficients, and the sequence $\{s_N(k)\}$ represents the coarser signal data at resolution level N, where $N=Ln_2(M)$. The second term is the wavelet expansion. The wavelet coefficients $C_j(k)$ can be interpreted as the local residual errors between successive signal approximations at scales j and $j+1$, and

$$r_j(t)=\sum_k C_j(k)\psi_{j,k}(t) \tag{6}$$

is the *detail signal* at scale j. It contains the information of the signal $S(t)$ corresponding to the frequencies $2^j\pi\leqslant|\omega|\leqslant 2^{j+1}\pi$. If the decomposition is carried out over all resolution levels, then the wavelet expansion will be

$$S(t)=\sum_{j=-N}^{-1}\sum_k C_j(k)\psi_{j,k}(t)=\sum_{j=-N}^{-1} r_j(t). \tag{7}$$

Since the family $\{\psi_{j,k}(t)\}$ is an *orthonormal* basis for $L^2(\mathbb{R})$, the concept of energy is linked with the usual notions derived from the Fourier theory. Then the wavelet coefficients are given by $C_j(k)=\langle S,\psi_{j,k}\rangle$, and the total energy by $\|S\|^2=\Sigma_{j<0}\Sigma_k|C_j(k)|^2$.

In the wavelet multiresolution framework (described above) it is possible to evaluate the energy corresponding to each level, and they can be used for the detection of the characteristic epileptic events [15]. Since we are using dyadic decomposition of the range of frequencies, from a signal of M samples, we have $M/2^{-j}$ coefficients at level j. In order to obtain an accurate event detection, we distribute the ''atoms'' of energy in each level j uniformly along 2^{-j} points. The energy in each resolution level $j=-1,\ldots,-N$, will be $E_j=\Sigma_k|C_j(k)|^2$, and the energy at each sampled time k will be $E(k)=\Sigma_{j=-N}^{-1}|C_j(k)|^2$.

Natural time series are usually combination of stochastic (noisy) and chaotic behaviors. Many applications, like nonlinear dynamics, require the separation of signal and noise [28,29]. Otherwise, when nonlinear invariants are evaluated (i.e., characteristic dimensions or Lyapunov exponents) the contaminating noise can give spurious results, and the obtained values will underestimate (if noise has strong periodic or almost periodic components) or overestimate (if noise is representative of a deterministic high dimensional or stochastic process) the real complexity of the system under study. When noise is present only in specific frequency bands, a filtering process can be implemented. However, from the point of view of nonlinear dynamics, filtering could be suitable only in some cases depending on the system under study. It is important to emphasize that a poorly designed filtering of the signal can give spurious results (i.e., filtering frequencies that determine the real dynamics of the signal).

Thus in these cases a filtering based on wavelet transform can be implemented in order to obtain a more accurate signal of the process under interest. Supposing, as in the case of tonic-clonic seizures, that we are interested in eliminating high frequency noise, using Eq. (7) at level j, the residual will be a smoothed version of the original signal, having fewer high frequencies in comparison to level $j+1$. This new signal will have half the data of the previous level; therefore, an interpolation with spline functions is applied in order to obtain the remaining data. On the other hand, interpolation by the cubic spline gives an efficient and very good approximation of the underlying physical signal given by samples [30]. Then this method can be accurately used for separation of noise, and the cleaned signal can be obtained as a sum of the interpolated residual components corresponding to the interesting frequency bands.

In summary, this method allows the elimination of nondesired frequency bands that hide other more interesting or unknown effects. Due to the orthogonality of the wavelet functions employed, we can be assured that only the unwanted and previously selected frequency bands were extracted, without needing to assume that linearity is necessary for making the traditional Fourier-based digital filtering.

B. Wavelet packets

As it is well known, wavelet analysis provides a *time-scale* description of any finite energy signal. Essentially, it is a successive decomposition of the signal in different scales. At each step, the corresponding details are separated, providing useful information for detecting and characterizing short time phenomena or abrupt changes of energy.

However, since wavelets do not possess a well defined average in frequency, they are not well suited to describe and characterize stationary phenomena or to detect time-frequency structures. This is an important limitation, because significant events often involve joint variations of time and frequency [24]. To overcome this problem, wavelet packet analysis appears as a natural extension of wavelet analysis. Moreover, this technique allows a time-scale-frequency description of the signals.

A family of wavelet packets is a collection of elemental signals obtained from appropriate linear combination of wavelets. They look like locally oscillating wave forms resembling modulated sines or cosines. Moreover, they can be organized on an orthonormal basis of the space of finite energy signals. The main advantage of using wavelet packets is that standard wavelet analysis can be extended with a flexible strategy. Thus, the description of the given signal can be well adapted according to the significant structures. Several families of wavelet packets have been proposed in the literature [16,24,27]. Here we will apply trigonometric spline wavelet packets [16]. First let us briefly review the proposed technique.

Given a finite energy signal $s_0(t)$, using spline wavelet analysis we can successively decompose them with the recursive scheme

$$s_{j+1}(t)=s_j(t)\oplus r_j(t) \tag{8}$$

for each scale $j=0,-1,\ldots,-N$. As already mentioned, the components $s_{j+1}(t)$ and $s_j(t)$ add to the information of the signal corresponding to the frequency bands $-2^{j+1}\pi\leqslant\omega\leqslant 2^{j+1}\pi$ and $-2^j\pi\leqslant\omega\leqslant 2^j\pi$, respectively. This means that the decomposition at level j consists of filtering the components $s_{j+1}(t)$, giving the details corresponding to the remaining frequencies $2^j\pi\leqslant|\omega|\leqslant 2^{j+1}\pi$. The component $r_j(t)$ adds to this information, and we can describe the signal $S(t)$ in term of detail signals as

$$S(t)=\sum_{j<0} r_j(t). \tag{9}$$

On the other hand, the detail components can be described in terms of wavelet atoms

$$r_j(t)\sum_k C_j(k)\psi_{j,k}(t). \tag{10}$$

Since each wavelet $\psi_{j,k}(t)=2^{j/2}\psi(2^jt-k)$ is well localized in the interval $2^{-j}k\leqslant t\leqslant 2^{-j}(k+1)$, the corresponding coefficient $C_j(k)$ adds to the local information of the detail. However, as we mentioned above, these coefficients average all the involved frequencies $2^j\pi\leqslant|\omega|\leqslant 2^{j+1}\pi$, and we will not gain explicit information about stationary structures.

Now we are interested in how to improve the frequency precision. The main idea is to decompose the components $r_j(t)$ in portions, each one covering a longer interval. Then we will locally implement an appropriate frequency technique.

We define any portion or local signal as

$$r_j^{(m,l)}(t)=\sum_{k=l}^{1+2^m-1} C_j(k)\psi_{j,k}(t), \tag{11}$$

where the parameters m and l are chosen in order that $r_j^{(m,l)}(t)$ covers the full time interval $2^{-j}l\leqslant t\leqslant 2^{-j}(l+2^m)$, which is a relatively long interval of length 2^{m-j}. Note that we defined the local wavelet packet with of 2^m basic functions $\psi_{j,k}(t)$ for $k=l,\ldots,l+2^m-1$.

Now, we define the set of fundamental frequencies

$$\omega_{mh}=\pi+2h\pi/2^m, \tag{12}$$

with $0\leqslant h\leqslant 2^{m-1}$, and associated the Fourier matrix $\mathbf{M}^{(m)}$ given by

$$M_{nk}^{(m)}=2^{-m/2}\begin{cases}\sin\left[\pi(k+1/2)\right] & \text{if } n=1\\ 2^{1/2}\cos\left[\omega_{mh}(k+1/2)\right] & \text{if } n \text{ is even}\\ 2^{1/2}\sin\left[\omega_{mh}(k+1/2)\right] & \text{if } n \text{ is odd}\\ \cos\left[2\pi(k+1/2)\right] & \text{if } n=2^m,\end{cases} \tag{13}$$

with $1\leqslant n\leqslant 2^m$, $0\leqslant k<2^m$ and $h=[[n/2]]$, where $[[\ ]]$ denotes the integer part. It can be demonstrated that $\mathbf{M}^{(m)}$ is a $2^m\times 2^m$ dimensional orthogonal matrix [16].

Then we can define the new set of elemental functions in order to expand $r_j^{(m,l)}(t)$ as a 2^m dimensional vector obtained from

$$\theta_{j,n}^{(m,l)}(t)=\sum_{k=l}^{1+2^m-1} M_{nk}^{(m)}\psi_{j,k}(t) \tag{14}$$

for $1\leqslant n\leqslant 2^m$.

Clearly, these functions constitute a new local orthonormal basis covering the interval under analysis, $2^{-j}l\leqslant t\leqslant 2^{-j}(l+2^m)$. Therefore we can give a second description of the local signal as

$$r_j^{(m,l)}(t)=\sum_{n=1}^{2^m} D_j^{(m,l)}(n)\,\theta_{j,n}^{(m,l)}(t). \tag{15}$$

The corresponding coefficients are easily computed as

$$D_j^{(m,l)}(n)=\sum_{k=l}^{l+2^m-1} M_{nk}^{(m)}C_j(k), \tag{16}$$

where $1\leqslant n\leqslant 2^m$.

The trigonometric wavelet packets $\theta_{j,n}^{(m,l)}(t)$ have zero mean, oscillate on the interval $2^{-j}l\leqslant t\leqslant 2^{-j}(l+2^m)$, and decay with exponential ratio. Moreover, their wave forms resemble modulate sines or cosines. In fact, it can be demonstrated that each Fourier transform $\hat{\theta}_{j,n}^{(m,l)}(\omega)$ is centered at the fundamental frequency ω_{mh}, when $n=2h$ or $n=2h$

$+1$. Moreover, $\hat{\theta}_{j,n}^{(m,l)}(\omega)=0$ on the other fundamental frequencies, and it has a fast decay outside the range $2^j\pi \leqslant|\omega|\leqslant 2^{j+1}\pi$.

In other words, the coefficients $\{D_j^{(m,l)}(n)\}$ can be considered as the discrete Fourier spectrum for the local signal $r_j^{(m,l)}(t)$. Summing up, in the double set of coefficients $\{C_j(k),D_j^{(m,l)}(n)\}$ we add to the time-scale-frequency information of the local signal $r_j^{(m,l)}(t)$.

Finally, to analyze the complete function $r_j(t)$, that is, the details at level j, we choose some partition in local components $r_j^{(m_i,l_i)}(t)$, according the structure of the signal,

$$r_j(t)=\sum_{m_i} r_j^{(m_i,l_i)}(t), \tag{17}$$

where the sequence of index l_i verifies $l_{i+1}=l_i+2^{m_i}$. Then we implement the time-scale-frequency technique for each local signal, referred to above.

C. Information cost function

Assuming that the given data series $S=\{s_0(n)\}$ has a finite energy, i.e.,

$$\sum_k |s_0(k)|<\infty \tag{18}$$

and $\Delta t=1$, we can approximate the energy of its spline representation in the form

$$\|S\|^2\cong\sum_k |s_0(k)|^2, \tag{19}$$

then the values

$$p_0(n)=|s_0(n)|^2 \Big/ \sum_n |s_0(n)|^2. \tag{20}$$

give the probability distribution of the signal's energy in the time domain.

Furthermore, in the wavelet multiresolution analysis of the time series $\{s_0(n)\}$, the energy in each resolution level j $(j<0)$ is the energy of the detail signal

$$E_j=\|r_j\|^2=\sum_k |C_j(k)|^2; \tag{21}$$

as a consequence, the total energy can be obtained by

$$E_{\text{tot}}=\|S\|^2=\sum_{j<0} E_j\,. \tag{22}$$

Then the normalized values

$$p_j=E_j/E_{\text{tot}}, \tag{23}$$

for $j=-1,-2,\ldots,-N$, define by scales the probability distribution of the energy. Clearly,

$$\sum_{j<0} p_j=\sum_n p_0(n)=1 \tag{24}$$

and the pair of distributions $(\{p_0(n)\},\{p_j\})$ can be considered as a time-scale density. They give a suitable tool for detecting and characterizing specific phenomena. The Shannon entropy gives a useful criteria for analyzing and comparing these distributions, since as is well known, it provides a measure of the information of any distribution.

We define the information cost function [17,18] as

$$\mathcal{C}_t=-\sum_n p_0(n)Ln_2[p_0(n)] \tag{25}$$

and

$$\mathcal{C}_\omega=-\sum_{j<0} p_jLn_2[p_j]. \tag{26}$$

The first function shows how redundant the time series is. In other words, it leads us to inquire whether the patterns are periodic phenomena. On the other hand, the second function shows the correlation between oscillating structures corresponding to different scales. In particular with this function self-similar processes can be detected.

It has become quite common in analyses of experimental time series with nonlinear systems to make a time delay reconstruction of the phase space in which the dynamic can be observed. The phase space portrait can be analyzed mathematically to demonstrate the existence of an attractor (the region of the phase space of lower dimension where the signal is confined in its future evolution) and its dimension [28,29]. A useful way to describe the dynamic behavior is to use Lyapunov exponents. These exponents measure the rate at which nearby points on an attractor diverge or converge along nearby trajectories [28,29]. We must emphasize that these metric parameters (dimensions, Lyapunov exponent, etc.) are defined only for stationary systems. In previous works, we confirmed, from a nonlinear dynamical analysis of epileptic EEG time series [10–12], the validity of the basic assumption that, at the seizure onset, a transition takes place in the dynamical behavior of the neural network from a complex behavior to a simpler one [6,8]. That means that, during an epileptic seizure the dimension of the attractor and the larger Lyapunov exponent present lower values compared with those evaluated at preseizure and post-seizure stages. Also the reconstructed attractor in phase space looks more simple and ordered.

The information cost function gives a measure of the order or disorder of the system in time. Thus, the ICF is a good parameter in order to detect dynamical changes in the system behavior, as well as a form of quantifying it [17,18]. The analysis of the ICF as a function of the different frequency bands and time shows in which bands the system has a tendency to order, or to a less chaotic behavior, during an epileptic seizure. In addition, the ICF has the following advantages over the following parameters: (i) over the entropy, because it is capable of detecting changes in a nonstationary signal due to the localization characteristics of the wavelet transform; (ii) over dimensions and Lyapunov exponents (which are only defined for stationary behaviors), because the computational time is significantly lower, since the algorithm involves the use of fast wavelet transforms in a multiresolution framework.

TABLE I. Frequency boundaries (in Hz) associated with the different resolution wavelet levels according with sample frequency $\omega_s = 102.4$ Hz. The traditional EEG frequency bands correspond to the following frequencies: δ (0.5–3.5 Hz); θ (3.5–7.5 Hz); α (7.5–12.5 Hz); β (12.5–30 Hz); γ (greater than 30 Hz).

Notation	$\omega_{\min}$	$\omega_{\max}$	Resolution level	EEG band
B_1	25.6	51.2	-1	γ, β
B_2	12.8	25.6	-2	β
B_3	6.4	12.8	-3	α, θ
B_4	3.2	6.4	-4	θ
B_5	1.6	3.2	-5	δ
B_6	0.8	1.6	-6	δ
B_7	0.4	0.8	-7	δ

IV. RESULT AND DISCUSSION

Orthogonal wavelet transform was used to analyze the scalp EEG signal corresponding to a tonic-clonic (TC) epileptic seizure. In Fig. 1 we show the signal. The seizure starts at second 10 with a discharge of slow waves superimposed by fast ones with lower amplitude. The tonic phase starts around second 35 with increasing amplitudes, and the clonic phase starts around second 50. The seizure finishes at second 85.

EEG spectral analysis is traditionally performed by studying different frequency bands, whose boundaries are well defined but could have some small variations according to the particular experiment being considered [1–3]. Absolute and relative intensities of these bands are analyzed and correlated with different pathologies. In this work, we chose seven frequency bands associated with resolution levels appropriate to the wavelet analysis in the scheme of multiresolution proposed. We denoted these band-resolution levels by B_j ($|j| = 1, \ldots, 7$), and their frequency limits, as well as their correspondence to traditional EEG frequency bands, are given in Table I.

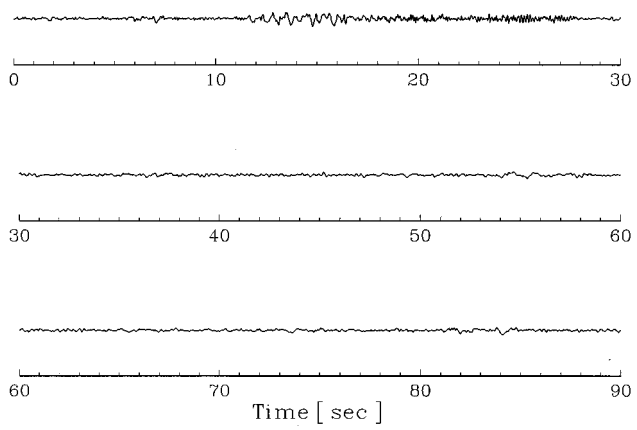

FIG. 2. Noise-free EEG signal. Same as Fig. 1, but without the fast frequencies (B_1 and B_2 bands).

Applying wavelet transform, we can filter the signal by subtracting the different bands. Figure 2 shows the smoothed time series corresponding to the signal of Fig. 1, where oscillations associated with the frequencies corresponding to B_1 and B_2 bands, with wavelet resolution level $j = -1$ and -2 respectively, were subtracted. For recovering the original sampling rate, this residual smoothed signal was interpolated with cubic splines. Owing to the fact that one of the goals of this work is to analyze middle and low frequency brain activity during an epileptic seizure, we eliminated B_1 and B_2 bands, both containing high frequency artifacts that obscure the EEG. Although high frequency brain activity will also be eliminated, it is well accepted that the components are not important in the study of an epileptic seizure [14,19,20].

We chose the frequency bands B_3 and B_4 for performing an analysis with wavelets packets, as was described in Sec. III. We selected these frequency bands because they carry the brain activity that is traditionally analyzed during an epileptic seizure. The series of $C_j(k)$ for $j = -3$ was segmented with a sliding windows of $l = 32$ samples corresponding to

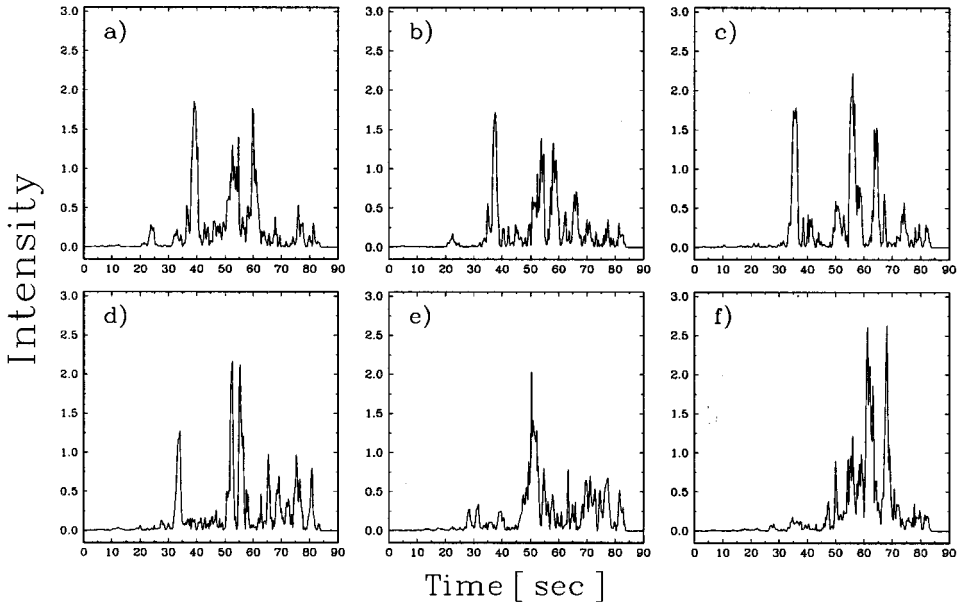

FIG. 3. Relevant wave packet intensities for the frequency band B_3 corresponding to the EEG signal displayed in Fig. 1. The wave packets are centered at the following frequencies: (a) 7.2 Hz, (b) 7.6 Hz, (c) 8.0 Hz, (d), 8.4 Hz, (e) 9.2 Hz, and (f) 10.8 Hz.

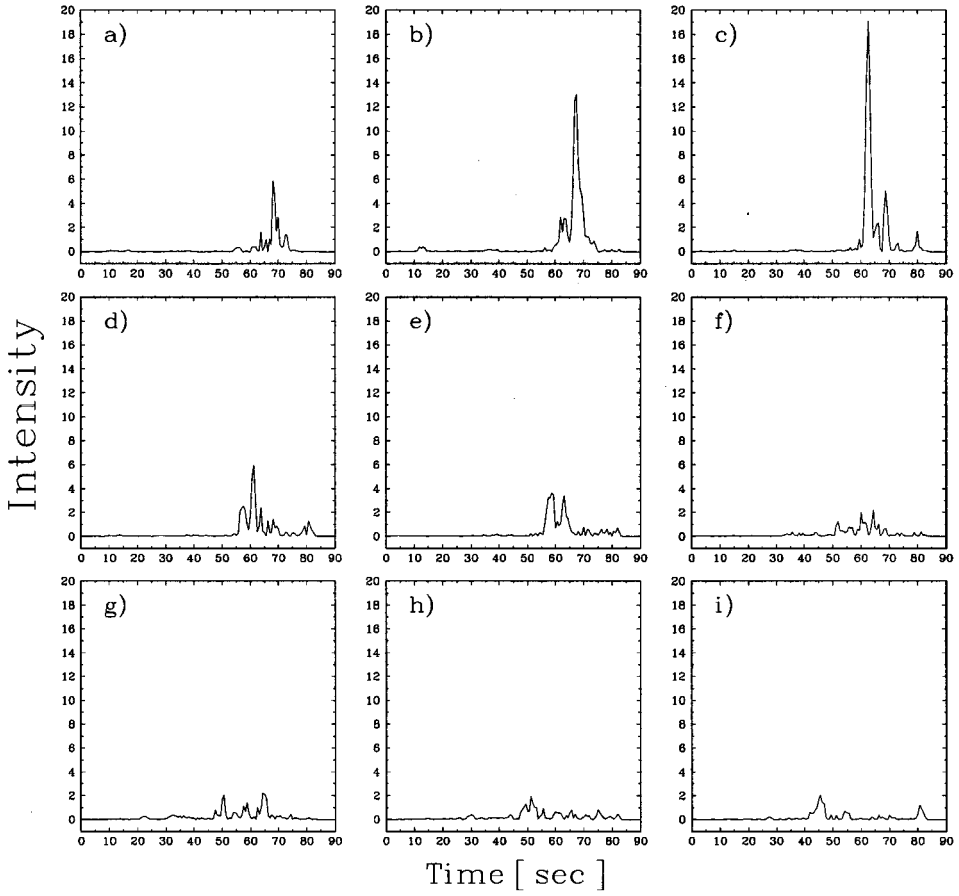

FIG. 4. Wave packet intensities for the frequency band B_4 corresponding to the EEG signal displayed in Fig. 1. The wave packets are centered at the following frequencies: (a) 3.2 Hz, (b) 3.6 Hz, (c) 4.0 Hz, (d) 4.4 Hz, (e) 4.8 Hz, and (f) 5.2 Hz, (g) 5.6 Hz, (h) 6.0 Hz, and (i) 6.4 Hz.

time intervals of $\Delta t = 2.5$ s. Discrete sets of $1 + l/2$ different frequencies between 6.4 and 12.8 Hz, with intervals of 0.4 Hz, were obtained.

Figure 3 shows wave packets of relevant amplitudes. They are centered at the frequencies (a) 7.2, (b) 7.6, (c) 8.0, (d) 8.4, (e) 9.2, and (f) 10.8 Hz. An important peak at second 35 can be identified in agreement with the starting of the tonic phase of the seizure, as was established by the physician team. It can be observed, mainly in the wave packets (b), (c), and (d), which means that its frequency structure can be decomposed mostly in these ranges. At 50 another peak indicates the starting of the clonic phase. It involves wave packets (d), (e), and (f). We can observe that the higher amplitudes in this band correspond to frequencies around 10 Hz, in agreement with previous works [14,19,20].

The same analysis for the B_4 band was achieved using $l = 16$ samples corresponding to time intervals of $\Delta t = 2.5$ s and discrete sets of frequencies between 3.2 and 6.4 Hz with intervals of 0.4 Hz. Note that the $j = -4$ level has half the dispersion in frequency compared with the $j = -3$ level (see Table I), and for this reason we used a window of 16 samples in order to obtain the same definition. These packets have a dispersion of ± 0.2 Hz. Figure 4 shows the amplitudes of wave packets centered in (a) 3.2, (b) 3.6, (c) 4.0, (d) 4.4, (e) 4.8, (f) 5.2, (g) 5.6, (h) 6, and (i) 6.4 Hz. The amplitudes of the corresponding wave packets show a peak around second 70, mainly in frequencies (b) and (c). This peak corresponds to a significant change in the morphology of the signal toward the end of the clonic phase of the seizure. This fact is in agreement with the low frequencies observed at the end of the seizure, and also mentioned in previous works [14,19,20].

The normalized energy as a function of time for the frequency bands $B_1 - B_7$ is shown in Fig. 5. An increase of the energy can be observed at the start of the seizure (10 s), and at the beginning of the tonic phase (35 s), and largest increase appears around second 50 with the start of the clonic stage. The largest increase of energy corresponds to the high frequencies concentrated in the B_1 and B_2 bands. The energy

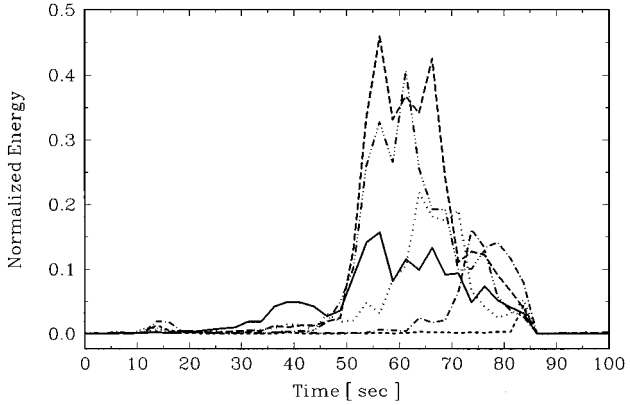

FIG. 5. Energy per band normalized to the total energy corresponding to the EEG signal displayed in Fig. 1, as a function of time. B_1 band (triple dot-dashed line), B_2 band (long dashed line), B_3 band (solid line), B_4 band (dotted line), B_5 band (dot-dashed line), and B_6 band (short dashed line). The B_7 band is not displayed because its values are almost zero for the considered interval.

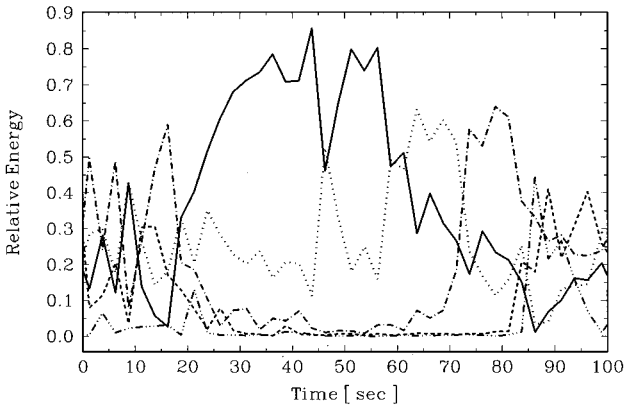

FIG. 6. Relative frequency band energy respect to the total energy, without the contribution of B_1 and B_2 bands. B_3 band (solid line), B_4 band (dotted line), B_5 band (dot-dashed line), B_6 band (short-dashed line), and B_7 band (triple-dot-dashed line).

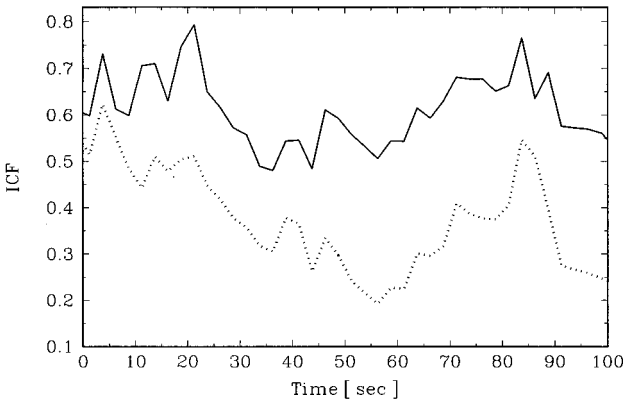

FIG. 7. Information cost function ICF (Shannon entropy) for the signal displayed in Fig. 1. The solid line represents the total ICF, and the dotted line is the same without the contribution of B_1 and B_2 bands.

of the B_3 band presents increasing values starting around seconds 35 and 50, in agreement with the beginning of the tonic and clonic phases, respectively. The energy of the B_4 band presents an increase in its values around second 65 (clonic phase). At this time a morphological change can be observed in the signal (see Fig. 1). The energy in the other frequency bands is low except in B_5, which presents an increment at the end of the seizure. In Fig. 6 we show the relative energy distribution among the frequency bands B_3-B_7, where the contribution of the frequency band B_1 and B_2 were removed from the total energy. We can observe in this figure that during an epileptic tonic-clonic seizure the dominant brain activity is concentrated in the B_3 and B_4 bands.

In summary, the above analysis shows that the energy is accumulated mainly in the fast frequencies during the tonic phase, and, when the seizure is ending, the slow and medium frequencies are the ones that become more relevant in the other stages. In conclusion, wavelet packets allow an identification of the dominant frequencies in each phase of the seizure, as well as a determination of the starting of each phase.

In Fig. 7 we display the total information cost function, and the ICF without the contributions of frequency bands B_1 and B_2, as a function of time. It is interesting to note that there is a remarkable decrease of the values at around second 35, corresponding to the beginning of the tonic phase, and then an increase around second 70, when the clonic phase of the seizure reaches its end. The observed decreasing values in the total ICF during the seizure could be associated with a more rhythmic behavior induced by the muscle activity, but, looking at the ICF without this kind of activity (B_1 and B_2 bands), we confirmed that the medium and low frequencies are also responsible for the signal order. This result confirms that the brain dynamical behavior during an epileptic seizure is more ordered than the preseizure and post-seizure stages.

V. CONCLUSIONS

With wavelet transform and derived methods, it is possible to clean an EEG signal in order to obtain dynamical parameters and hidden frequency information. These noisy EEG signals are usually neglected by physicians.

The analysis carried out in a tonic-clonic epileptic seizure using wavelet transform and wave packets has shown that, during an epileptic seizure, the relevant brain activity presents frequencies around 10 Hz, and when the seizure nears completely the brain activity become slower, with frequencies around 4 Hz. High frequency muscle activity obscures the signal. These high frequencies are the ones that accumulate energy during the tonic phase of the seizure.

The peaks observed while performing wave packet analyses in B_3 and B_4 bands establish with accurate precision the starting and the ending of the different phases of the TC seizure. They also mark changes in the signal morphology that could be correlated with the clinical symptomatology. The analysis of the total energy, relative energy, and ICF as functions of time shed light on the dynamical process or tendency to order during the seizure. These changes only can be actually observed through the video-EEG.

Several numerical methods were developed for describing the EEG signal in the time-frequency domain. Orthogonal wavelet transform appears to be very convenient, due to its capability for separating different frequency bands without modifying the remanent ones. It is specially straightforward for analyzing brain activity information. Moreover, this method is suitable for studying the energy accumulation and its exchange among the different frequency bands at different stages of the seizure. The dynamic of the seizure can also be accessed by performing an analysis based on the information cost function, showing at which stage and in which frequency band a less chaotic behavior is involved.

ACKNOWLEDGMENTS

This work was partially supported by the Consejo Nacional de Investigaciones Científicas y Técnicas (CONICET, Argentina) and the International Office of BMBF, Germany. The authors wish to thank H. Garcia and A. Rabinowicz of the Instituto de Investigaciones Neurológicas Raúl Carra (FLENI), Argentina, for useful comments, and for providing the EEG recordings used in this work.

[1] *Handbook of Electroencephalography and Clinical Neurophysiology, Vol. I: Methods of Analysis of Brain Electrical and Magnetic Signals*, edited by A. Gevins and A. Rémond (Elsevier, Amsterdam, 1987).

[2] *Handbook of Electroencephalography and Clinical Neurophysiology, Vol. II: Clinical Applications of Computer Analysis of EEG and Other Neurophysiological Signals*, edited by F. H. Lopes da Silva, Storm van Leeuwen, and A. Rémond (Elsevier, Amsterdam, 1986).

[3] *Electroencephalography, Basic Principles, Clinical Applications, and Related Field*, edited by E. Niedermeyer and F. H. Lopes da Silva (Urban and Schwarzenberg, Baltimore, 1987).

[4] *Current Practice of Clinical Electroencephalography*, 2nd ed. edited by D. D. Daly and T. A. Pedley (Reven, New York, 1990).

[5] A. Babloyantz, in *Dimensions and Entropies in Chaotic Systems*, edited by G. Meyer-Kress (Springer-Verlag, Berlin, 1986), pp. 241–245.

[6] *Chaos in Brain Function*, edited by Erol Başar (Springer-Verlag, Berlin, 1990).

[7] S. C. Layne, G. Meyer-Kress, and J. Holzfuss, in *Dimensions and Entropies in Chaotic Systems* (Ref. [5]), pp. 246–256.

[8] B. J. West, in *Fractal Physiology and Chaos in Medicine, Nonlinear Phenomena in Life Science*, edited by B. J. West (World Scientific, Singapore, 1990).

[9] S. Blanco, H. García, R. Quian Quiroga, L. Romanelli, and O. A. Rosso, IEEE Eng. Med. Biol. Mag. **14**, 395 (1995).

[10] S. Blanco, S. Kochen, R. Quian Quiroga, L. Riquelme, O. A. Rosso, and P. Salgado, in *Wavelet Theory and Harmonic Analysis in Applied Sciences*, edited by E. M. Fernandez-Berdaguer and C. E. D'Attellis (Birkhäuser, Boston, 1997), pp. 179–226.

[11] S. Blanco, A. Figliola, S. Kochen, and O. A. Rosso, IEEE Eng. Med. Biol. Mag. **16**, 83 (1997).

[12] S. Blanco, R. Quian Quiroga, O. A. Rosso, and S. Kochen, Phys. Rev. E **51**, 2624 (1995).

[13] S. Blanco, S. Kochen, O. A. Rosso, and P. Salgado, IEEE Eng. Med. Biol. Mag. **16**, 316 (1997).

[14] R. Quian Quiroga, S. Blanco, O. A. Rosso, H. Garcia, and A. Rabinowicz, Electromyogr Clin. Neurophysiol. (to be published).

[15] S. Blanco, C. D'Attellis, S. Isaacson, O. A. Rosso, and R. Sirne, Phys. Rev. E **54**, 6661 (1996).

[16] E. Serrano, Ph.D. thesis, FCEyN, Universidad de Buenos Aires, 1996.

[17] A. Figliola, E. Serrano, IEEE Eng. Med. Biol. Mag. **16**, 74 (1997).

[18] A. Figliola and C. Baredes, in *Instabilities and Nonequilibrium structures VI*, edited by E. Tirapegui and W. Zeller (Kluwer, Dordrecht, in press).

[19] H. Gastaut and R. Broughton (unpublished).

[20] J. Gotman, J. R. Ives, and P. Gloor, Clin. Neurophysiol. **52**, 626 (1981).

[21] Y. Meyer, *Ondelettes and Operateurs* (Hermann, Paris, 1990), Books I–III.

[22] C. K. Chui, *An Introduction to Wavelets* (Academic, San Diego, 1992).

[23] I. Daubechies, *Ten Lectures on Wavelets* (SIAM, Philadelphia, 1992).

[24] Y. Meyer, *Wavelets, Algorithms and Applications* (SIAM, Philadelphia, 1993).

[25] M. Unser, A. Aldroubi, and M. Eden, Signal Process. **30**, 141 (1993).

[26] *Wavelets in Medicine and Biology*, edited by A. Aldroubi and M. Unser (CRC, Boca Raton, 1996).

[27] R. R. Coifman (unpublished).

[28] H. D. I. Abarbanel, R. Brown, J. J. Sidorowich, and L. Sh. Tsimring, Rev. Mod. Phys. **65**, 1331 (1993).

[29] H. D. I. Abarbanel, *Analysis of Observed Chaotic Data* (Springer-Verlag, New York, 1995).

[30] J. J. Shoemberg, *Cardinal Spline Interpolation* (SIAM, Philadelphia, 1993).